HHS Public Access

Author manuscript

J Neuroimaging. Author manuscript; available in PMC 2023 September 01.

Published in final edited form as:

J Neuroimaging. 2022 September ; 32(5): 866–874. doi:10.1111/jon.13040.

Identification of association fibers using ex vivo diffusion tractography in Alexander disease brains

Tadashi Shiohama[1,a], **Natalie Stewart**[2], **Masahito Nangaku**[3], **Andre J.W. van der Kouwe**[4], **Emi Takahashi**[1,b,c]

[1]Division of Newborn Medicine, Department of Medicine, Boston Children's Hospital, Harvard Medical School, 300 Longwood Avenue, Boston, MA 02115, USA

[2]College of Science, Northeastern University, Boston, MA 02115, USA

[3]Chiba University School of Medicine, Chiba 2608677, Japan

[4]Athinoula A. Martinos Center for Biomedical Imaging, Department of Radiology, Massachusetts General Hospital, Charlestown, MA 02144, USA

Abstract

Background and Purpose: Alexander disease (AxD) is a neurodegenerative disorder caused by heterozygous Glial Fibrillary Acidic Protein mutation. The characteristic structural findings of AxD, such as leukodystrophic features, are well known, while association fibers of AxD remain uninvestigated. The aim of this study was to explore global and subcortical fibers in four brains with AxD using ex vivo diffusion tractography.

Methods: High-angular resolution diffusion magnetic resonance imaging (HARDI) tractography and diffusion-tensor imaging (DTI) tractography were used to evaluate long and short association fibers and compared to histological findings in brain specimens obtained from four donors with AxD and two donors without neurological disorders.

Results: AxD brains showed impairment of long association fibers, except for the arcuate fasciculus and cingulum bundle, and abnormal trajectories of the inferior longitudinal and fronto-occipital fasciculi on HARDI tractography and loss of multi-directionality in subcortical fibers on DTI tractography. In histological studies, AxD brains showed diffuse low density on Klüver–Barrera and neurofilament staining and sporadic Rosenthal fibers on hematoxylin and eosin staining.

Conclusions: This study describes the spatial distribution of degenerations of short and long association fibers in AxD brains using combined tractography and pathological findings.

Corresponding author: Tadashi Shiohama, Department of Pediatrics, Chiba University Hospital, 1-8-1 Inohana, Chuo-ku, Chiba-shi, Chiba 260-8677, Japan, Tel.: +81(43)226-2144, Fax: +81(43)226-2145, asuha_hare@yahoo.co.jp.

[a]Current addresses of authors
Department of Pediatrics, Chiba University Hospital, Chiba 2608677, Japan

[b]Athinoula A. Martinos Center for Biomedical Imaging, Department of Radiology, Massachusetts General Hospital, Charlestown, MA 02144, USA

[c]Department of Radiology, Harvard Medical School, Boston, MA 02144, USA

Keywords

Alexander disease; Diffusion-tensor imaging; High-angular resolution diffusion MRI; Association fibers; Post-mortem; Histology

Introduction

Alexander disease (AxD) is a rare but devastating disease that affects neural development and causes ataxia, seizures, intellectual dysfunction, and many other disabilities.[1,2] It is caused by heterozygous pathogenic variants of the Glial Fibrillary Acidic Protein (GFAP),[3–5] which codes for a major intermediate filament protein expressed exclusively in astrocytes within the brain. GFAP-null mice display only subtle neuropathology,[6] while mice with knock-in AxD-linked mutant human GFAP[7] or significant overexpression of wild-type human GFAP[8,9] replicate brain pathological features of AxD, suggesting that GFAP mutation in AxD acts in a gain-of-function fashion.

The pathologic hallmark of AxD is an abundance of Rosenthal fibers (RFs), an inclusion body composed of aggregates of aberrant GFAP and several other proteins within astrocytes.[3,4,10–12] GFAP accumulates in astrocytes of mice,[13] zebrafish,[14] and flies[15] with induced human GFAP and in patients with AxD.[16,17] In addition to RF formation, pathological features of AxD include widespread demyelination and astrocyte dysfunction.[10–12,18] RFs are characteristic to AxD but also found in astrocytoma[19,20] and reactive gliosis.[21–25] Therefore, AxD is a rare congenital disorder and a potential model of primary astrocytic disorders.[26]

The critical mechanism connecting GFAP aggregation in astrocytes and neurotoxicity remains poorly understood. Nevertheless, mechanosensitive signaling activation by changes in brain matrix stiffness,[27] inflammatory conditions, such as microglia activation and T-cell infiltration,[8,28] activation of autophagy,[16] and excitotoxic neuronal death induced by a loss of glutamate buffering[29,30] have been reported as pathological mechanisms of compromised astrocytes causing the neurodegenerative disorder. Although reducing mutant GFAP protein, which may cause RFs, might have therapeutic potential,[31,32] no cure has been found for AxD to date, and treatments are still palliative.

Exploring short and long association fibers is crucial for evaluating brain morphology in congenital disorders because disconnection of the cerebral regions by white matter damage produces the same results as impairment of those cerebral regions.[33] Particularly, ex vivo diffusion magnetic resonance imaging (MRI) has advantages over in vivo diffusion MRI in terms of a high signal-to-noise ratio and spatial resolution.[34] Although some neuroimaging studies have reported MRI features, particularly leukodystrophic features, of AxD,[2] to the best of our knowledge, no study has assessed brain pathways in AxD. Therefore, little is known about brain connectivity in AxD. In this study, we explored global and subcortical fibers using ex vivo diffusion MRI tractography in four brains with AxD and two brains without neurological disorders (hereafter referred to as “non-AxD”).

Although diffusion MRI tractography cannot distinguish axons, glial fibers, and aligned cell components, it is potentially superior to histology in demonstrating global fiber connections. The aim of this study was to reveal impaired patterns of global connectivity in AxD, which are not identified by histological studies, using diffusion MRI tractography.

Methods

Specimens and preparation for scans

This study was conducted in accordance with the tenets of the Declaration of Helsinki. The study protocol was approved by the Boston Children's Hospital. Brain specimens from four AxD (Table 1) and two non-AxD patients were obtained from the University of Maryland Brain and Tissue Bank (http://medschool.umaryland.edu/btbank). Informed consent for brain donation was obtained before death from the patient or after death from the family members. Brains of AxD and non-AxD groups were extracted en-bloc from the skull, hemisected, and immersed in 10% formalin. We obtained the right hemicoronal slabs of the four AxD brains and the whole left hemisphere of one non-AxD brain. We scanned three fixed slabs in each case to compare matched brain regions across patients, along with the whole hemisphere. Brain specimens were stored in 4% formalin and placed in individual plastic bags with Fomblin oil during MRI scanning, as described previously.[35,36] Clinical and autopsy information was provided by the Brain Bank (Table 2).

Diffusion MRI scanning and processing

Diffusion-weighted data were acquired over two averages using a steady-state free-precession-based diffusion sequence (repetition time, 24.82 ms; echo time, 18.76 ms; $\alpha = 60°$),[36,37] using a 3-Tesla MRI machine (TIM Trio, Siemens, Germany) with a 32-channel head coil. The imaging matrix was 200 × 400 × 200 for four slabs and 176 × 128 × 192 for the left hemisphere. Slab thickness was 192 mm with 240 slices (800-μm slices, 200 × 200 matrix, 160 × 160-mm field-of-view). Diffusion weighting was performed along 44 directions ($b = 1{,}500$ s/mm^2) with four images with b of 0. Scanning was performed at the Athinoula A. Martinos Center for Biomedical Imaging.

We used Diffusion Toolkit and TrackVis (http://trackvis.org) to reconstruct/visualize pathways using the streamline algorithm (http://trackvis.org). An angle threshold of 45° was employed for this study because there tends to be too many clearly erroneous tractography pathways at 60° and too few reasonable tracts (e.g., callosal pathways) at 35°. Trajectories were propagated by pursuing the orientation vector of least curvature. Color-coding of fibers was based on a standard red–green–blue code, applied to the vector between the endpoints of each fiber (red for right–left, green for dorsal–ventral, and blue for anterior–posterior).

Diffusion tractography for detecting cortical association fibers

In a hemisected AxD brain (AxD 1, Figure 1) and its control, we identified and visualized six major cortico-cortical pathways (Figure 2), i.e., the arcuate fasciculus (AF), inferior longitudinal fasciculus (ILF), inferior fronto-occipital fasciculus (IFOF; only in control), uncinated fasciculus (UF), cingulum bundle (CB), and fornix (Fx), as in previous studies,[38–41] using high-angular resolution diffusion MRI (HARDI)[42] with the following

parameters: 60 directions (plus 5 b = 0 volumes), 45° angle threshold, no fractional anisotropy mask, and 0.65-mm isotropic spatial resolution.

Anatomic and tractography atlases[38,40,41] were used to guide region of interest (ROI) placements on mean diffusion-weighted images to delineate pathways of interest.[43,44] Two neuroscientists confirmed ROI placements and resulting courses of fiber pathways. For the CB and Fx pathways, several ROIs were placed along the white matter regions for each pathway shown in the atlases. For the ILF, IFOF, and UF pathways, two ROIs were used in the destination of each pathway: anterior temporal and occipital regions for ILF, inferior frontal and occipital regions for IFOF, and inferior frontal and anterior temporal regions for UF. The size of all ROIs was carefully optimized in the control data to exclude other white matter pathways and not miss the pathways of interest by changing their size and location several times. In addition, we explored abnormal trajectories of ILF and IFOF in AxD 1 by changing the size and location of ROIs from the original (Figure 3).

The subcortical pathways were identified in the hemicoronal slabs of the brain specimens from AxD patients (AxD 1–4) and a donor without neurological disorders (non-AxD 1 and 2) using diffusion-tensor imaging (DTI) tractography (Figure 4).[35,36]

Histological staining

To compare images of DTI tractography and histology, we dissected slabs after MRI (Figure 5). Histological processing was performed at Boston Children's Hospital. After being processed for immunohistochemistry, brain specimens of AxD 1–4 and non-AxD 3, were cryoprotected in 10% and then 30% sucrose phosphate buffer before being sectioned coronally at 20 μm on a freezing microtome, saving every section. Klüver–Barrera stain (KB; combined cresyl violet stain for Nissl bodies and Luxol fast blue stain for myelin), neurofilament stain (NF) for axons, and hematoxylin and eosin stain (H&E) specific to RFs were used. Staining of neurotypical control procedures followed literature protocols.[45–47] The neurofilament light polypeptide antibody (2F11, Cell Marque, Rocklin, CA) was used for NF.

Results

Diffusion tractography for detecting cortical association fibers

HARDI tractography of the left hemisphere of AxD 1 clearly identified the thalamocortical, ILF, and many short-range corticocortical pathways (Figure 1). Parts of AF and UF were also detected. Frontal lobe-specific ventriculomegaly was observed with significant cortical thinning and severely affected fiber pathways (Figure 1). Volumes of the fiber pathways in UF, Fx, ILF, and IFOF were decreased, while those in AF and CB were relatively preserved (Figure 2). In non-AxD 1, these six major cortico-cortical pathways were clearly identified (Figure 2).

We identified the IFOF anteriorly (Figure 3, yellow pathways), the optic radiation pathways (Figure 3, pink pathways) that ran along the IFOF, and a part of the posterior pathways of the IFOF in AxD 1 (Figure 3, yellow pathways in AxD 1). Such pathways in AxD 1 took a different course than the optic radiation near the lateral geniculate nucleus (Figure

3, yellow arrows in AxD 1), in good agreement with the IFOF trajectory in non-AxD cases (Figure 3, yellow arrows in non-AxD 1). The frontal subcortical atrophy in AxD 1 extended posteriorly, and the disconnected IFOF pathways terminated at a posterior edge of the extended frontal atrophy (Figure 3, red arrow in AxD 1) at the posterior limit of the insular subcortical area (Figure 3, red arrow in non-AxD 1).

After the occipital ROI was moved anteriorly, more ILF pathways were detected (Figure 3, blue pathways, light blue arrow), most of which connected with the anterior medial temporal lobe in AxD 1 (Figure 3, dark blue arrow) and the lateral temporal regions in non-AxD 1 (Figure 3, green arrow).

Local subcortical pathways

DTI tractography of neurotypical controls showed multidirectional fibers. In non-AxD cases, DTI fibers with multiple directions were identified (Figure 4, non-AxD 1 and 2). In cases of juvenile and adult AxD, volumes of left–right or anterior–posterior directional DTI fibers were decreased, while those of radially directional fibers were clearly preserved (Figure 4, white arrows in AxD 2–4).

Histological findings

In all AxD cases, we observed extensively decreased white matter densities with KB and NF and sporadic RFs with H&E (Figure 6). Histological studies in non-AxD 3 showed no abnormal findings (Figure 6).

Discussion

The current study described the spatial distribution of degeneration of short and long association fibers in AxD using combined diffusion MRI tractography and pathological findings. HARDI tractography in the left hemisphere of an infantile AxD case showed sparing of long association fibers running through the periventricular region, such as the AF and CB. DTI tractography showed decreased volume predominantly in left–right or anterior–posterior directional fibers of short cortico-cortical pathways, while radially directional fibers were clearly preserved. Histological studies detected diffuse low density on KB and NF staining and sporadic RFs on H&E staining in AxD. Although these findings were consistent with the typical pathological findings of AxD, they were not useful in identifying the spatial distribution of axonal impairment in AxD.

This study included one case of infantile AxD (AxD 1) and three cases of juvenile or adult AxD (AxD 2–4). The infantile case (AxD 1) showed a huge cystic lesion in the frontal lobe and impairment of cortico-cortical association pathways. Short cortico-cortical pathways (shown as blue fiber in Figure 4) were relatively persistent compared to those of juvenile and adult AxD. Whether the difference in DTI tractography findings between AxD brains depends on the clinical type or age at scanning remains unclear. Impairment of short cortico-cortical pathways may be associated with a long-standing mild GFAP accumulation in late-onset types (juvenile and adult forms) of AxD.

Severity of compromised astrocytes and accumulation of RFs (or GFAP) in AxD displays spatial distribution on pathological findings,[30] i.e., the subpial cortex, deep white matter, cerebellar white matter, and white matter tracts of the brain stem and spinal cord involve enlarged astrocytes with RFs, while the isocortex and subcortical white matter are relatively spared from RF accumulation.[30] In contrast, the spatial distribution of axonal impairment in AxD has not been reported. The results of our study showed that subcortical association fibers were impaired more severely than peripheral radial directional fibers at least on diffusion MR tractography, despite the unclear demonstration of astrocyte impairment in subcortical regions in the pathological assessment.

HARDI and DTI for detecting association fasciculi

HARDI tractography uses multidirectional water diffusivity to detect crossing pathways with better discrimination within image voxels,[42] even in immature brains with more unmyelinated or hypomyelinated fibers compared to adult brains.[48–50] HARDI has an advantage over DTI of detecting multiple directions of water diffusivity within a voxel, which could help identify long traverse pathways through multiple brain regions. Therefore, we used HARDI tractography for detecting association fasciculi in the whole hemisphere.

Although traditional DTI typically allows only the detection of one direction of water diffusivity per voxel,[51] it has an advantage of detecting pathways with continuous trajectories curving with angles above the given angle.[36] It tends to determine more coherent tractography pathways than HARDI in the tissue if the same number of diffusion gradient directions is used. The slabs we scanned tended to show lower signal-to-noise ratios than the whole hemisphere sample. Therefore, we used DTI tractography for detecting local cortico-cortical fibers in the brain slabs.

Because we used relatively low b-values, measures from HARDI and DTI in this study possibly did not significantly differ. In addition, we did not compare HARDI results from one group and DTI results from the other group. We compared tractography results across groups either using HARDI or DTI.

Limitations

This study has several limitations due to its preliminary nature. Ex vivo diffusion MRI allows visualization of very high-resolution water diffusivity from which coherent fiber pathways can be inferred, but we cannot directly distinguish which diffusion MR tractography pathways represent axons, glial fibers, or aligned cell components. This limitation is part of the nature of current diffusion MRI studies, and histology is superior to MRI in terms of spatial resolution and directness. However, histology has a different type of limitation, which precludes the study of global fiber connections. Confirmation of the biological accuracy of HARDI with optimal scanning and analysis parameters could advance the field of whole-brain non-invasive connectional neuroanatomy, and we have actively worked on this topic.[52–54] Since AxD has not been extensively studied, assessing the brain pathology in AxD to better understand and potentially classify the clinical course of the disease could be beneficial. In addition, AxD brains can elucidate the pathologic correlates of DTI findings. Although many studies conducted histological correlation of DTI, what can

be observed on diffusion MRI in AxD with regional astrocyte abnormalities is unknown. An additional limitation is that causes of death in AxD and non-AxD cases vary. Matching the cause of death is challenging since in most cases of diseased brains, the cause of death is regarded as "complications of disorder," which is not what we expect in a control.

Future directions

The current study is the first step towards the understanding of local and global brain pathology in AxD and has great potential for future studies, which could lead to better prediction of the clinical course of brain pathologies in AxD. Since in vivo MRI has a lower spatial resolution than ex vivo MRI, confidently assessing abnormal fiber pathways in the brain in vivo is difficult. Careful assessment of ex vivo DTI and histology would provide the basis for in vivo DTI (e.g., in vivo pathways would likely be "true" pathways if ex vivo DTI also reported the same fiber patterns). We have compared ex and in vivo DTI for brain disorders and often observed similar abnormal fiber patterns. The next step of this study would be to perform DTI for AxD in vivo, and the results could be informative for the study of AxD and other axonal/glial degenerative brain disorders.

In addition, astrocyte dysfunction is recognized as a key developmental mechanism of neurodegeneration in several diseases, including AD,[55] PD,[56] Huntington's disease,[57] amyotrophic lateral sclerosis,[58] epilepsies,[59] and multiple sclerosis,[60] as well as AxD. Although most of these diseases are complex syndromes including dysfunctions in neurons and immune cells, astrocyte dysfunction is thought to be an important aspect of such diseases.[31] Therefore, understanding the AxD pathology can lead to understanding of many other neurological diseases.

In conclusion, our study using ex vivo diffusion MR tractography in AxD revealed in detail the spatial distribution of impairments of long and short association fibers, which was not previously identified by histological studies. These impaired patterns of global connectivity in AxD may contribute to a better understanding of the pathogenic mechanism of cognitive disfunction in AxD. Evaluation of spatial distribution of axonal impairment using diffusion MR tractography is potentially applicable for other primary astrocytic disorders.[26]

Acknowledgments and Disclosure

We thank Dr. Hart G.W. Lidov for providing histological staining images in normal control and Elizabeth Ethier for proofreading a previous version of this paper. We thank Editage (http://www.editage.com) for editing and reviewing this manuscript in English. The authors declare no conflict of interest.

Funding

This research project was supported by National Institute of Neurological Disorders and Stroke (NINDS) R03NS101372 to E.T. and JSPS KAKEN (JP21K07694) to T.S.

References

1. Srivastava S, Naidu S. Alexander Disease. In: Gene Reviews. Available at: http://www.ncbi.nlm.nih.gov/books/NBK1172. Accessed January 10, 2022.
2. Tavasoli A, Armangue T, Ho CY, et al. Alexander Disease. J Child Neurol 2017;32:184–7. [PubMed: 28112050]

3. Brenner M, Johnson AB, Boespflug-Tanguy O, et al. Mutations in GFAP, encoding glial fibrillary acidic protein, are associated with Alexander disease. Nat Genet 2001;27:117–20. [PubMed: 11138011]
4. Li T, Johnson AB, Salomons G, et al. Glial fibrillary acidic protein mutations in infantile, juvenile, and adult forms of Alexander disease. Ann Neurol 2005;57:310–26. [PubMed: 15732097]
5. Bonthius DJ, Karacay B. Alexander Disease: A novel mutation in GFAP leading to epilepsia eartialis continua. J Child Neurol 2016;31:869–72. [PubMed: 26719496]
6. McCall MA, Gregg RG, Behringer RR, et al. Targeted deletion in astrocyte intermediate filament (Gfap) alters neuronal physiology. Proc Natl Acad Sci U S A 1996;93:6361–6. [PubMed: 8692820]
7. Hagemann TL, Connor JX, Messing A. Alexander disease-associated glial fibrillary acidic protein mutations in mice induce Rosenthal fiber formation and a white matter stress response. J Neurosci 2006;26:11162–73. [PubMed: 17065456]
8. Hagemann TL, Gaeta SA, Smith MA, Johnson DA, Johnson JA, Messing A. Gene expression analysis in mice with elevated glial fibrillary acidic protein and Rosenthal fibers reveals a stress response followed by glial activation and neuronal dysfunction. Hum Mol Genet 2005;14:2443–58. [PubMed: 16014634]
9. Cho W, Messing A. Properties of astrocytes cultured from GFAP over-expressing and GFAP mutant mice. Exp Cell Res 2009;315:1260–72. [PubMed: 19146851]
10. Jacob J, Robertson NJ, Hilton DA. The clinicopathological spectrum of Rosenthal fibre encephalopathy and Alexander's disease: a case report and review of the literature. J Neurol Neurosurg Psychiatry 2003:74:807–10. [PubMed: 12754360]
11. Der Perng M, Su M, Wen SF, et al. The Alexander disease-causing glial fibrillary acidic protein mutant, R416W, accumulates into Rosenthal fibers by a pathway that involves filament aggregation and the association of alpha B-crystallin and HSP27. Am J Hum Genet 2006;79:197–213. [PubMed: 16826512]
12. Wippold FJ 2nd, Perry A, Lennerz J. Neuropathology for the neuroradiologist: Rosenthal fibers. AJNR Am J Neuroradiol 2006;27:958–61. [PubMed: 16687524]
13. Messing A, Head MW, Galles K, Galbreath EJ, Goldman JE, Brenner M. Fatal encephalopathy with astrocyte inclusions in GFAP transgenic mice. Am J Pathol 1998;152:391–8. [PubMed: 9466565]
14. Lee SH, Nam TS, Kim KH, et al. Aggregation-prone GFAP mutation in Alexander disease validated using a zebrafish model. BMC Neurol 2017;17:175. [PubMed: 28882119]
15. Wang L, Colodner KJ, Feany MB. Protein misfolding and oxidative stress promote glial-mediated neurodegeneration in an Alexander disease model. J Neurosci 2011;31:2868–77. [PubMed: 21414908]
16. Tang G, Yue Z, Talloczy Z, et al. Autophagy induced by Alexander disease-mutant GFAP accumulation is regulated by p38/MAPK and mTOR signaling pathways. Hum Mol Genet 2008;17:1540–55. [PubMed: 18276609]
17. Sosunov AA 2nd, McKhann GM, Goldman JE. The origin of Rosenthal fibers and their contributions to astrocyte pathology in Alexander disease. Acta Neuropathol Commun 2017;5:27. [PubMed: 28359321]
18. Wang L, Hagemann TL, Kalwa H, Michel T, Messing A, Feany MB. Nitric oxide mediates glial-induced neurodegeneration in Alexander disease. Nat Commun 2015;6:8966. [PubMed: 26608817]
19. Cyrine S, Sonia Z, Mounir T, et al. Pilocytic astrocytoma: a retrospective study of 32 cases. Clin Neurol Neurosurg 2013;115:1220–5. [PubMed: 23265563]
20. Smith DA, Lantos PL. Immunocytochemistry of cerebellar astrocytomas: with a special note on Rosenthal fibres. Acta Neuropathol 1985;66:155–9. [PubMed: 2861704]
21. Singh G, Tatke M. Rosenthal fibers and eosinophilic granular bodies in an acoustic schwannoma. Indian J Pathol Microbiol 2011;54:629–31. [PubMed: 21934245]
22. Ertan Y, Sarsik B, Ozgiray E, Kitis O, Dalbasti T, Akalin T. Pigmented ependymoma with signet-ring cells and Rosenthal fibers: a rare variant of ependymoma. Neuropathology 2010;30:71–5. [PubMed: 19508348]

23. Cillekens JM, Beliën JA, van der Valk P, et al. A histopathological contribution to supratentorial glioma grading, definition of mixed gliomas and recognition of low grade glioma with Rosenthal fibers. J Neurooncol 2000;46:23–43. [PubMed: 10896203]
24. Khanlou N, Mathern GW, Mitchell WG, et al. Cortical dysplasia with prominent Rosenthal fiber formation in a case of intractable pediatric epilepsy. Hum Pathol 2009;40:1200–4. [PubMed: 19427021]
25. Kupsky WJ, Frosch M. Tuberous sclerosis variant with production of Rosenthal fibers (alpha B-crystallin). Pediatr Pathol 1993;13:869–73. [PubMed: 8108304]
26. Olabarria M, Goldman JE. Disorders of astrocytes: Alexander disease as a model. Annu Rev Pathol 2017;12:131–52. [PubMed: 28135564]
27. Wang L, Xia J, Li J, et al. Tissue and cellular rigidity and mechanosensitive signaling activation in Alexander disease. Nat Commun 2018;9:1899. [PubMed: 29765022]
28. Olabarria M, Putilina M, Riemer EC, Goldman JE. Astrocyte pathology in Alexander disease causes a marked inflammatory environment. Acta Neuropathol 2015;130:469–86. [PubMed: 26296699]
29. Tian R, Wu X, Hagemann TL, et al. Alexander disease mutant glial fibrillary acidic protein compromises glutamate transport in astrocytes. J Neuropathol Exp Neurol 2010;69:335–45. [PubMed: 20448479]
30. Sosunov A, Olabarria M, Goldman JE. Alexander disease: an astrocytopathy that produces a leukodystrophy. Brain Pathol 2018;28:388–98. [PubMed: 29740945]
31. Messing A, Brenner M, Feany MB, Nedergaard M, Goldman JE. Alexander disease. J Neurosci 2012;32:5017–23. [PubMed: 22496548]
32. Wang L, Hagemann TL, Messing A, Feany MB. An in vivo pharmacological screen identifies cholinergic signaling as a therapeutic target in glial-based nervous system disease. J Neurosci 2016;36:1445–5. [PubMed: 26843629]
33. Filley CM, Fields RD. White matter and cognition: making the connection. J Neurophysiol 2016;116:2093–104. [PubMed: 27512019]
34. Vasung L, Charvet CJ, Shiohama T, Gagoski B, Levman J, Takahashi E. Ex vivo fetal brain MRI: Recent advances, challenges, and future directions. Neuroimage 2019;195:23–37. [PubMed: 30905833]
35. Takahashi E, Dai G, Wang R, et al. Development of cerebral fiber pathways in cats revealed by diffusion spectrum imaging. Neuroimage 2010;49:1231–40. [PubMed: 19747553]
36. Wilkinson M, Wang R, van der Kouwe A, Takahashi E. White and gray matter fiber pathways in autism spectrum disorder revealed by ex vivo diffusion MR tractography. Brain Behav 2016;6:e00483. [PubMed: 27247853]
37. McNab JA, Miller KL. Sensitivity of diffusion weighted steady state free precession to anisotropic diffusion. Magn Reson Med 2008;60:405–413. [PubMed: 18666106]
38. Catani M, Thiebaut de Schotten M. A diffusion tensor imaging tractography atlas for virtual in vivo dissections. Cortex 2008;44:1105–32. [PubMed: 18619589]
39. Cohen AH, Wang R, Wilkinson M, MacDonald P, Lim AR, Takahashi E. Development of human white matter fiber pathways: From newborn to adult ages. Int J Dev Neurosci 2016;50:26–38. [PubMed: 26948153]
40. Thiebaut de Schotten M, Ffytche DH, Bizzi A, et al. Atlasing location, asymmetry and inter-subject variability of white matter tracts in the human brain with MR diffusion tractography. Neuroimage 2011;54:49–59. [PubMed: 20682348]
41. Mori S, Tournier JD. Introduction to diffusion tensor imaging and higher order models (1st edition). Cambridge, MA: Academic Press; 2013:93–123.
42. Tuch DS, Reese TG, Wiegell MR, Makris N, Belliveau JW, Wedeen VJ. High angular resolution diffusion imaging reveals intravoxel white matter fiber heterogeneity. Magn Reson Med 2002;48:577–82. [PubMed: 12353272]
43. Shiohama T, Chew B, Levman J, Takahashi E. Quantitative analyses of high angular resolution diffusion imaging (HARDI)-derived long association fibers in children with sensorineural hearing loss. Int J Dev Neurosci 2020;80:717–29. [PubMed: 33067827]

44. Catani M, Thiebaut de Schotten M. A diffusion tensor imaging tractography atlas for virtual in vivo dissections. Cortex 2008;44:1105–32. [PubMed: 18619589]
45. Brody BA, Kinney HC, Kloman AS, Gilles FH. Sequence of central nervous system myelination in human infancy. I. An autopsy study of myelination. J Neuropathol Exp Neurol 1987;46:283–301. [PubMed: 3559630]
46. Kinney HC, Filiano JJ. Brainstem research in sudden infant death syndrome. Pediatrician 1988;15:240–50. [PubMed: 3068663]
47. Folkerth RD, Alroy J, Bhan I, Kaye EM. Infantile G (M1) gangliosidosis: complete morphology and histochemistry of two autopsy cases, with particular reference to delayed central nervous system myelination. Pediatr Dev Pathol 2000;3:73–86. [PubMed: 10594135]
48. Takahashi E, Folkerth RD, Galaburda AM, Grant PE. Emerging cerebral connectivity in the human fetal brain: an MR tractography study. Cereb Cortex 2012;22:455–64. [PubMed: 21670100]
49. Takahashi E, Hayashi E, Schmahmann JD, Grant PE. Development of cerebellar connectivity in human fetal brains revealed by high angular resolution diffusion tractography. Neuroimage 2014;96:326–33. [PubMed: 24650603]
50. Wilkinson M, Lim AR, Cohen AH, Galaburda AM, Takahashi E. Detection and growth pattern of arcuate fasciculus from newborn to adult. Front Neurosci 2017;11:389. [PubMed: 28769741]
51. Frank LR. Characterization of anisotropy in high angular resolution diffusion-weighted MRI. Magn Reson Med 2002;47:1083–99. [PubMed: 12111955]
52. Xu G, Takahashi E, Folkerth RD, et al. Radial coherence of diffusion tractography in the cerebral white matter of the human fetus: neuroanatomic insights. Cereb Cortex 2014;24:579–92. [PubMed: 23131806]
53. Wang R, Dai G, Takahashi E. High resolution MRI reveals detailed layer structures in early human fetal stages: in vitro study with histologic correlation. Front Neuroanat 2015;9:150. [PubMed: 26834575]
54. Vasung L, Raguz M, Kostovic I, Takahashi E. Spatiotemporal relationship of brain pathways during human fetal development using high-angular resolution diffusion MR imaging and histology. Front Neurosci 2017;11:348. [PubMed: 28744187]
55. Cai Z, Wan CQ, Liu Z. Astrocyte and Alzheimer's disease. J Neurol 2017;264:2068–74. [PubMed: 28821953]
56. Booth HDE, Hirst WD, Wade-Martins R. The role of astrocyte dysfunction in Parkinson's disease pathogenesis. Trends Neurosci 2017;40:358–70. [PubMed: 28527591]
57. Khakh BS, Beaumont V, Cachope R, Munoz-Sanjuan I, Goldman SA, Grantyn R. Unravelling and exploiting astrocyte dysfunction in Huntington's disease. Trends Neurosci 2017;40:422–37. [PubMed: 28578789]
58. Pehar M, Harlan BA, Killoy KM, Vargas MR. Role and therapeutic potential of astrocytes in amyotrophic lateral sclerosis. Curr Pharm Des 2017;23:5010–21. [PubMed: 28641533]
59. Boison D, Steinhäuser C. Epilepsy and astrocyte energy metabolism. Glia 2018;66:1235–43. [PubMed: 29044647]
60. Ludwin SK, Rao VT, Moore CS, Antel JP. Astrocytes in multiple sclerosis. Mult Scler 2016;22:1114–24. [PubMed: 27207458]

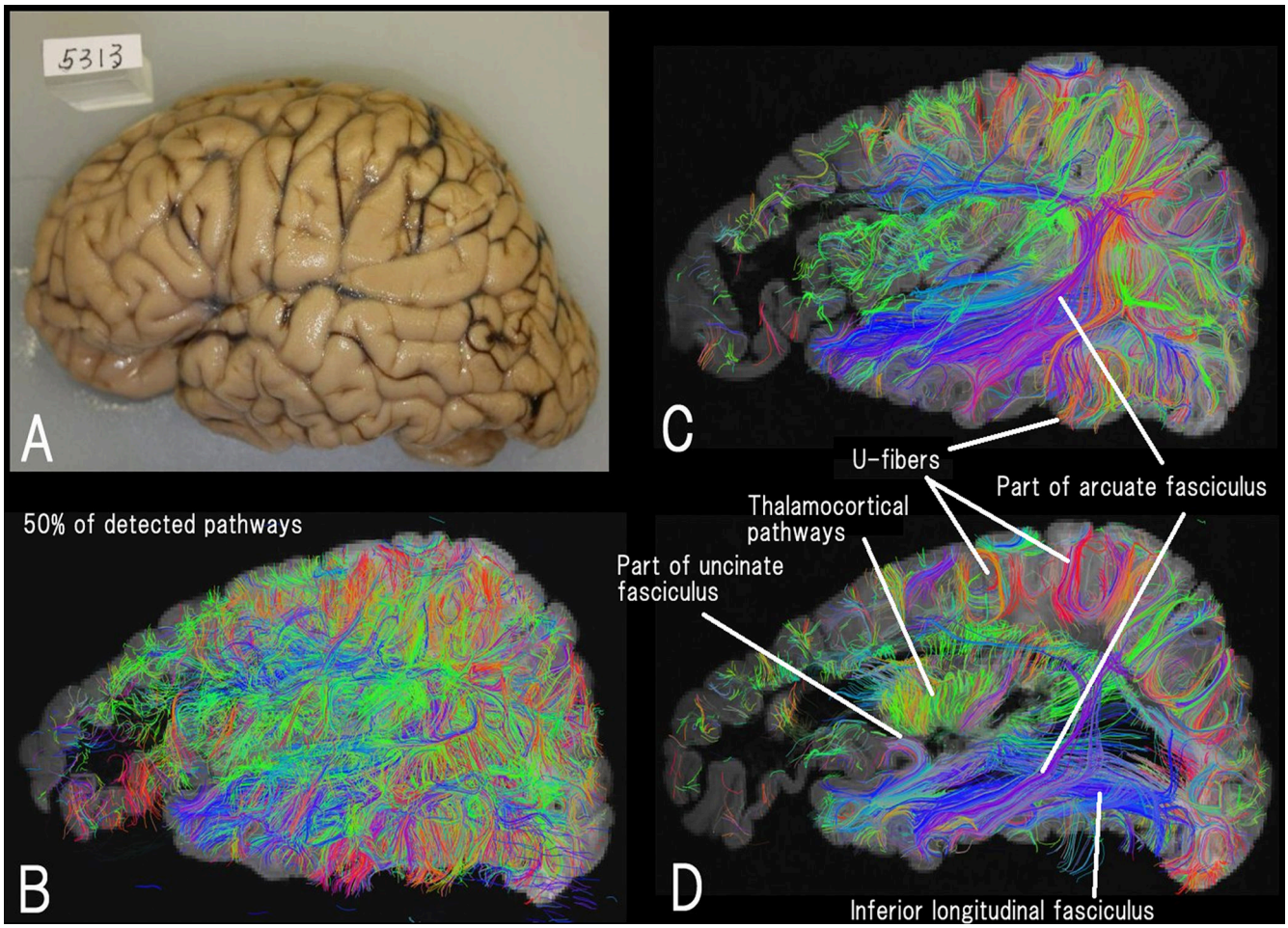

Figure 1.

High-angular resolution diffusion MRI tractography of the left hemisphere (A) of a 7-year-old boy with Alexander disease (B–D). Different levels of sagittal views of 50% of detected fiber pathways are shown. The thalamocortical, inferior longitudinal fasciculus, and many short-range cortico-cortical (u-fiber) pathways are clearly imaged. Parts of the arcuate and uncinated fasciculi are also detected. Color-coding of fibers is based on the standard red–green–blue code, applied to the vector between the endpoints of each fiber (red for right–left, green for dorsal–ventral, and blue for anterior–posterior).

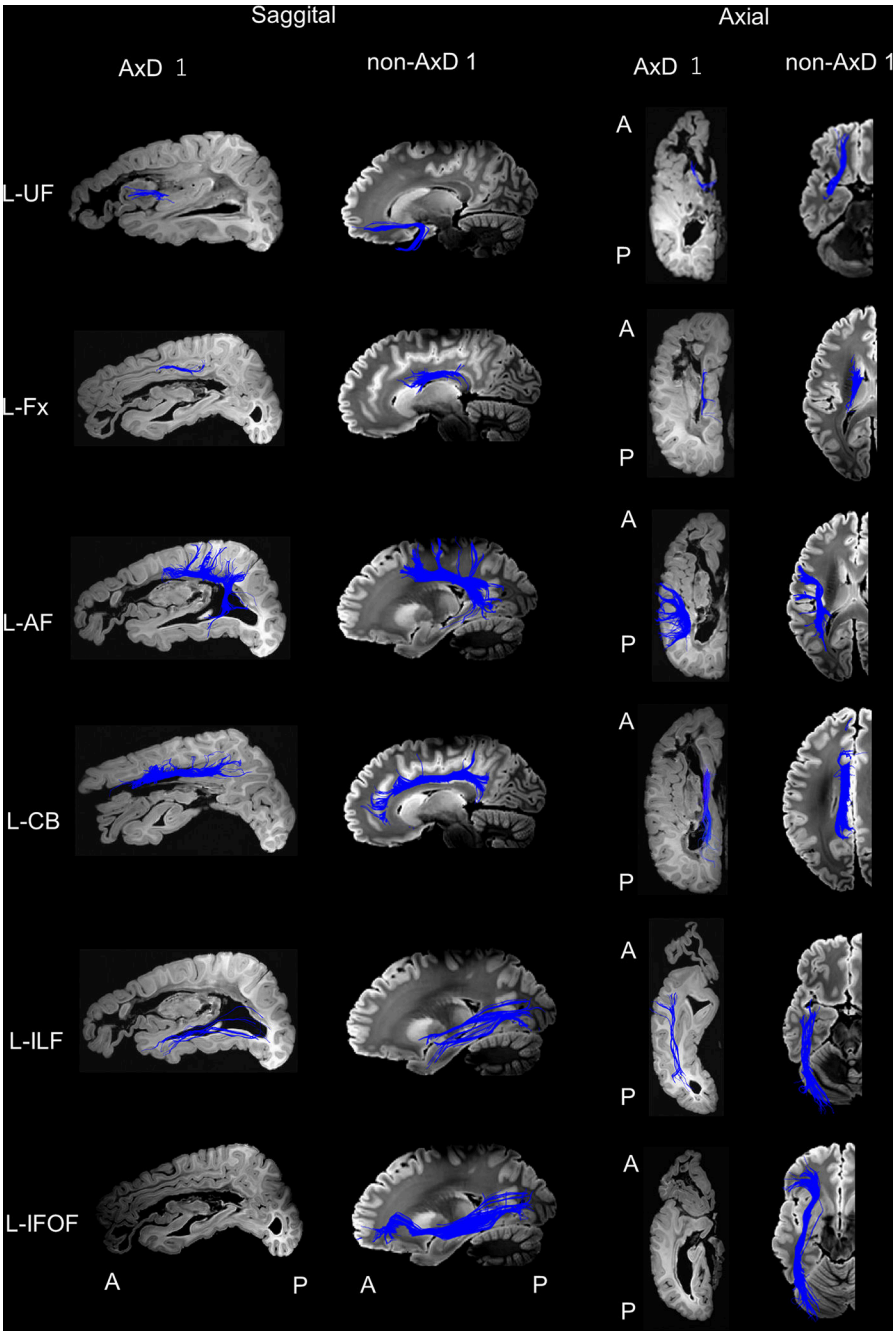

Figure 2.

High-angular resolution diffusion MRI tractography showing major cortico-cortical pathways of the left hemisphere of a 9-year-old boy with Alexander disease (AxD 1) and a 9-year-old neurotypical boy (non-AxD 1). Abbreviations: A, anterior; AF, arcuate fasciculus; CB, cingulum bundle; Fx, fornix; IFOF, inferior fronto-occipital fasciculus; ILF, inferior longitudinal fasciculus; L, left; P, posterior; UF, uncinated fasciculus.

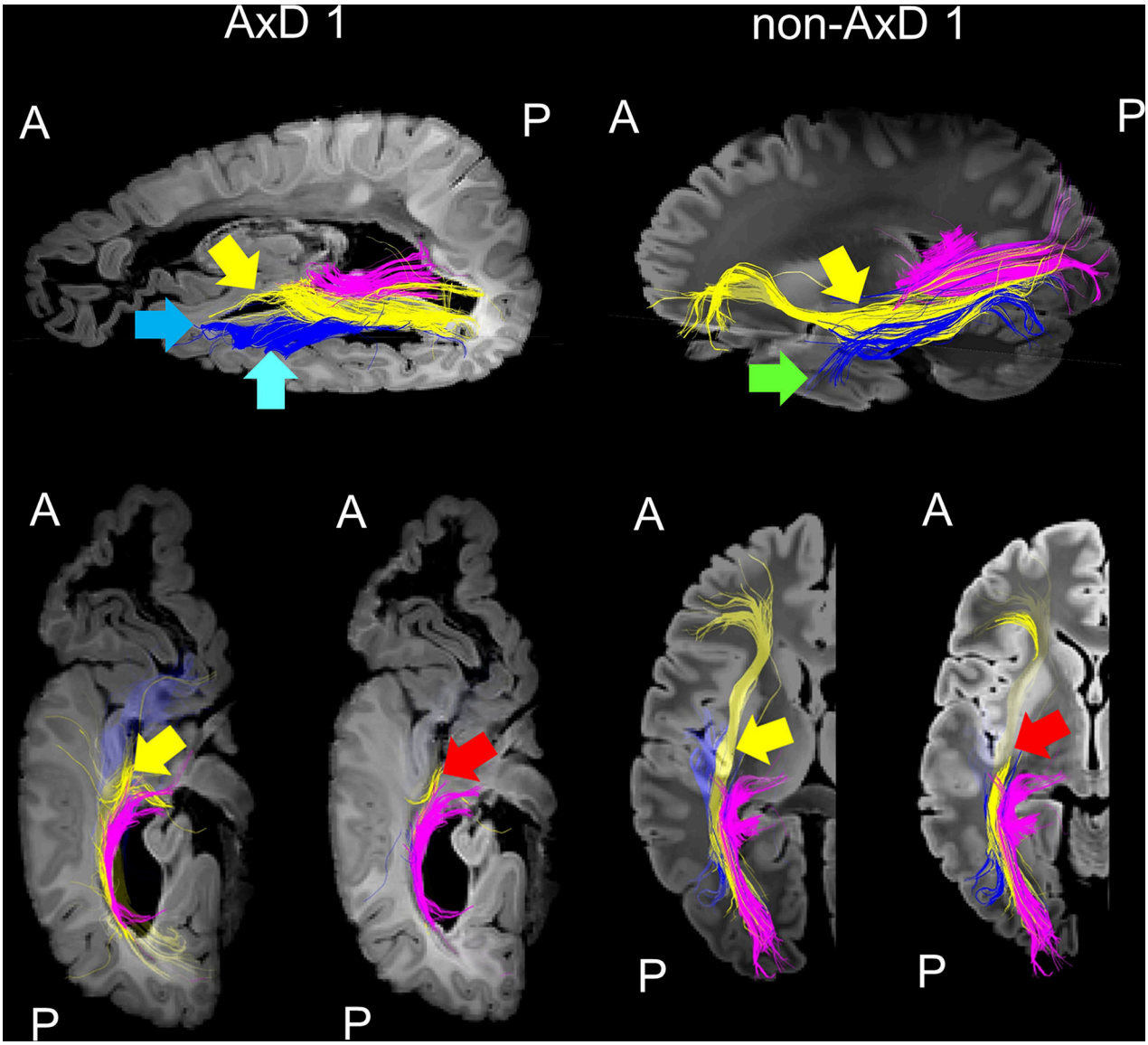

Figure 3.

High-angular resolution diffusion MRI tractography of the left hemisphere of a 9-year-old boy with Alexander disease (AxD 1) and a 9-year-old neurotypical boy (non-AxD 1). The optic radiation pathways (pink pathways), inferior fronto-occipital fasciculus (yellow pathways, yellow arrows, dark blue arrow, red arrows), and inferior longitudinal fasciculus (blue pathways, green arrow, light blue arrow) are visualized. Abbreviations: A, anterior; P, posterior.

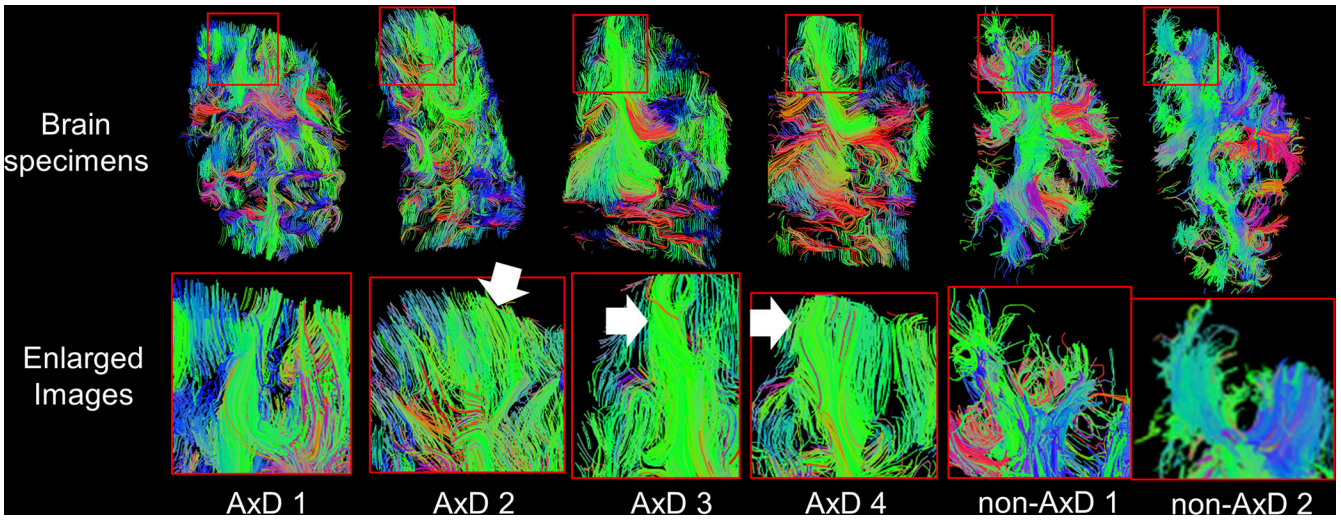

Figure 4.

Diffusion-tensor imaging tractography in cases of Alexander disease (AxD 1–4) and neurotypical controls (non-AxD 1, 9 years old; non-AxD 2, 19 years old). Upper and lower panels showing coronal slabs at the level of the thalamus and enlarged views of the right superior frontal cortex, respectively. Color-coding of fibers is based on the standard red–green–blue code, applied to the vector between the endpoints of each fiber (red for right–left, green for dorsal–ventral, and blue for anterior–posterior). White arrows indicate radially directional fibers.

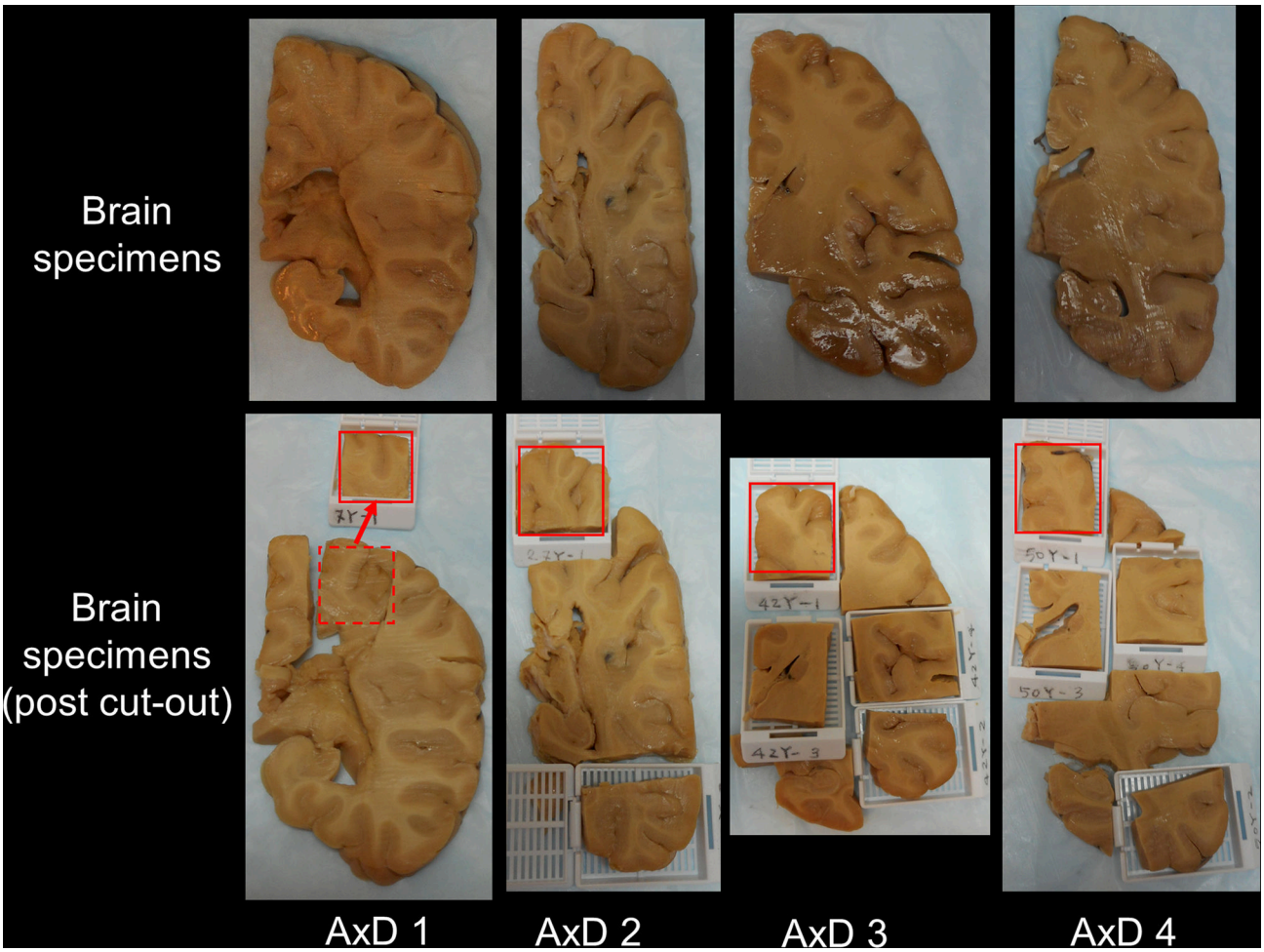

Figure 5.
Brain specimens of coronal slabs at the level of the thalamus (pre- and post-cutoff) in cases of Alexander disease (AxD 1–4).

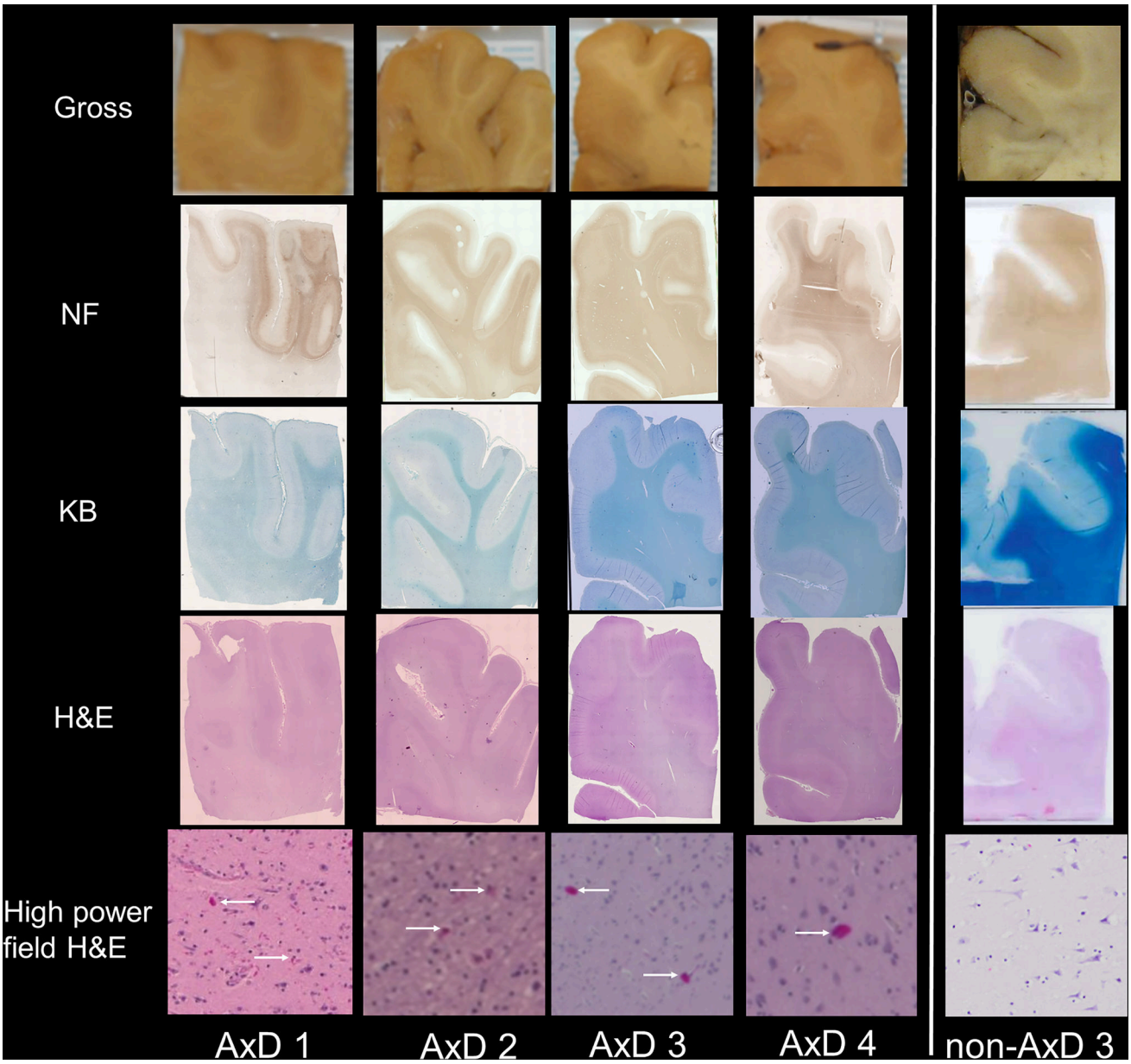

Figure 6.

Histological findings in the right superior frontal cortex in cases of Alexander disease (AxD 1–4) and a neurotypical control (non-AxD 3). White arrows indicate the Rosenthal fibers. Abbreviations: H&E, Hematoxylin–Eosin stain; KB, Klüver–Barrera stain; NF, neurofilament stain.

Table 1

Clinical information of donors of the Alexander disease brains

	AxD 1	AxD 2	AxD 3	AxD 4
Age of death	7 years	27 years	42 years	50 years
Sex	Male	Female	Female	Female
AxD type	Infantile	Juvenile	Adult	Adult
Clinical symptoms	Profound developmental delay, epilepsy, hypothyroidism, constipation, dysphagia, failure to thrive	Intellectual disability, clumsiness, epilepsy, spasticity, progressive cognitive dysfunction	Generalized weakness, gait ataxia, fatigue, profound family history	Migraine, ataxic gait, nystagmus, intellectual dysfunction, depression, hydrocephalus
In vivo MRI findings	Cystic lesions in the frontal lobes and cerebellum	Cerebral leukodystrophy	Encephalomalacia in the frontal lobe	Hydrocephaly, cerebellar white matter lesions
Pathological findings	RF deposits	RF deposits	RF deposits	RF deposits
Genetic tests	N.D.	GFAP p.K63E	N.D.	N.D.

Abbreviation: AxD, Alexander disease; RF, Rosenthal fiber; MRI, magnetic resonance imaging; N.D., not described

Table 2

Clinical background and preservation of brain tissue after death in both groups

	Brain age (years)	Disease	Sex	Race	Post-mortem interval (h)	Time in fixative (years)
AxD 1	7	AxD	Male	Hispanic	14	7.25
AxD 2	27	AxD	Female	Caucasian	22	7.5
AxD 3	42	AxD	Female	Caucasian	4	9.5
AxD 4	50	AxD	Female	Caucasian	17	11
Non-AxD 1	9	Died from asphyxia	Female	African–American	8	13
Non-AxD 2	19	Died from multiple injuries	Male	Caucasian	14	10
Non-AxD 3	15	Died from complications of a systemic illness not involving the nervous system	Male	N.A.	40	N.A. (no MRI scan)

Abbreviation: AxD, Alexander disease; non-AxD, donors without neurological disorders; N.A., not available; h: hours